The molecular evolution of feathers with direct evidence from fossils

Yanhong Pan[a,1], Wenxia Zheng[b], Roger H. Sawyer[c], Michael W. Pennington[d], Xiaoting Zheng[e,f], Xiaoli Wang[e,f], Min Wang[g,h], Liang Hu[a,i], Jingmai O'Connor[g,h], Tao Zhao[a], Zhiheng Li[g,h], Elena R. Schroeter[b], Feixiang Wu[g,h], Xing Xu[g,h], Zhonghe Zhou[g,h,1], and Mary H. Schweitzer[b,j,1]

[a]Chinese Academy of Sciences Key Laboratory of Economic Stratigraphy and Palaeogeography, Nanjing Institute of Geology and Palaeontology and Center for Excellence in Life and Paleoenvironment, Chinese Academy of Sciences, Nanjing 210008, China; [b]Department of Biological Sciences, North Carolina State University, Raleigh, NC 27695; [c]Department of Biological Sciences, University of South Carolina, Columbia, SC 29205; [d]AmbioPharm Incorporated, North Augusta, SC 29842; [e]Institute of Geology and Paleontology, Lingyi University, Lingyi City, 27605 Shandong, China; [f]Shandong Tianyu Museum of Nature, Pingyi, 273300 Shandong, China; [g]CAS Key Laboratory of Vertebrate Evolution and Human Origins of the Chinese Academy of Sciences, Institute of Vertebrate Paleontology and Paleoanthropology, Chinese Academy of Sciences, 100044 Beijing, China; [h]Center for Excellence in Life and Paleoenvironment, Chinese Academy of Sciences, 100044 Beijing, China; [i]College of Earth and Planetary Sciences, University of Chinese Academy of Sciences, 100049 Beijing, China; and [j]North Carolina Museum of Natural Sciences, Raleigh, NC 27601

Dinosaur fossils possessing integumentary appendages of various morphologies, interpreted as feathers, have greatly enhanced our understanding of the evolutionary link between birds and dinosaurs, as well as the origins of feathers and avian flight. In extant birds, the unique expression and amino acid composition of proteins in mature feathers have been shown to determine their biomechanical properties, such as hardness, resilience, and plasticity. Here, we provide molecular and ultrastructural evidence that the pennaceous feathers of the Jurassic nonavian dinosaur *Anchiornis* were composed of both feather β-keratins and α-keratins. This is significant, because mature feathers in extant birds are dominated by β-keratins, particularly in the barbs and barbules forming the vane. We confirm here that feathers were modified at both molecular and morphological levels to obtain the biomechanical properties for flight during the dinosaur–bird transition, and we show that the patterns and timing of adaptive change at the molecular level can be directly addressed in exceptionally preserved fossils in deep time.

feather evolution | keratin expression | fossil-feather ultrastructure | dinosaur–bird transition | biomechanical properties

Feathers are a key avian feature, used to identify and diagnose birds in the fossil record for centuries. The appearance of feathers has been closely tied to the origin of flight in birds. Although feathers have been used as a taxonomic character of birds, discoveries of fossils from Middle-Late Jurassic to Early Cretaceous sediments in western Liaoning, northern Hebei, and Inner Mongolia of China have revealed a remarkable diversity of nonavian dinosaur fossils displaying a wide range of integumentary appendages interpreted as feathers or feather-like structures (1–4). Some of these structures are present as simple filamentous structures without aerodynamic function, and these are widespread in more basal and flightless dinosaurs, including some ornithischians not on the bird lineage (4–6). This distribution supports the hypothesis that feathers may have originated before the capacity for powered flight and, thus, were first employed for other purposes.

Complex pennaceous feathers with rachises and branching barbs and barbules have been described on the tail and limbs of Middle-Late Jurassic paravian dinosaurs, the best known among them being *Anchiornis* (3). *Anchiornis* represents a taxon that is significantly older (~160 Ma) (7) than the first recognized bird, *Archaeopteryx* (~150–155 Ma) (8), but strongly resembles it. The skeletal and feather anatomy, small body size, and long forelimbs (3, 9, 10) of *Anchiornis* suggest volant abilities, which is supported by anatomy-based computer models and wind-tunnel studies (11). However, although the pennaceous structure is confirmed for

feathers in *Anchiornis*, barbules that interlock to form feather vanes critical for flight have not been identified yet (12).

In addition to morphological features, the ultrastructure and molecular composition are critical in determining whether the mechanical properties of feathers are suitable for flight (13, 14). Mature feathers of extant birds are primarily composed of β-keratins, a family of proteins found only in birds and reptiles (15). However, α-keratins, as a more basal protein family found in all vertebrates (16, 17), are coexpressed with derived β-keratins in the embryonic feathers of extant birds (15, 17) and in all other sauropsid keratinous tissues.

In mammals, α-keratins can be divided into "hard" (hair, nails, hooves) and "soft" (skin) keratins based on the number of intra- and intermolecular cross-links (14). Sauropsid-specific β-keratins are universally harder, because they incorporate a greater number of sulfur-bearing amino acids, which form stabilizing cross-links and form β-sheets as opposed to helices, as in α-keratins (14). The β-keratins in extant birds are further divided into subfamilies (e.g., basal claw and scale β-keratin subfamilies) (14, 18), and the more derived feather β-keratins. The latter are distinguished by a peptide deletion, resulting in the loss of the glycine-rich tail in

---

Significance

During the dinosaur–bird transition, feathers of bird ancestors must have been molecularly modified to become biomechanically suitable for flight. We report molecular moieties in fossil feathers that shed light on that transition. Pennaceous feathers attached to the right forelimb of the Jurassic dinosaur *Anchiornis* were composed of both feather β-keratins and α-keratins, but were dominated by α-keratins, unlike mature feathers of extant birds, which are dominated by β-keratins. Data suggest that the pennaceous feathers of *Anchiornis* had some, but not all, of the ultrastructural and molecular characteristics of extant feathers, and may not yet have attained molecular modifications required for powered flight.

the C-terminal region, a shorter amino acid sequence and, as a consequence, lower molecular weight, than other avian β-keratins (14, 18). This deletion creates a structural protein that is biomechanically more flexible, imparting to avian feathers the unique properties required for flight (16, 17, 19–23).

The ultrastructure and molecular composition of the pennaceous feathers in *Anchiornis* may, therefore, shed light on the controversial issue (24) of its volant behavior. We argue that unless the pennaceous feathers of *Anchiornis* exhibit a molecular composition dominated by specific feather β-keratins, they were unlikely to support powered flight.

Molecular clock studies have suggested that feather β-keratins began to diverge from other β-keratins by ~143 Ma (95% SD ~ 176–110 Ma) (23). These studies supported the hypothesis that pennaceous feathers preceded flight, and led to the prediction that *Anchiornis* (~160 Ma) expressed only more basal β-keratins, but not the derived feather β-keratins identified in extant birds.

To test this hypothesis and to determine the distribution of keratins across the dinosaur–bird transition, we employed multiple high-resolution analytical methods and strict controls (including various extant tissues) to elucidate the endogenous preservation and molecular expression of keratins in fossilized feathers. We compared pennaceous feathers attached to the forelimb of *Anchiornis* with fossil feathers from taxa that are phylogenetically more derived than *Anchiornis* (e.g., pennaceous feathers possibly from the left forelimb of an Early Cretaceous Dromaeosauridae indet., wing feathers of the right forelimb of *Eoconfuciusornis*, tail feathers near the distal end of the left pubis of *Yanornis*, and an isolated Oligocene flight feather). As controls, we included short fibers around the perimeter of the bones of the Late Cretaceous *Shuvuuia deserti* (a nonavian dinosaur) and claw sheath material from the Late Cretaceous *Citipati* (a nonavian dinosaur), as well as modern comparable tissues, including flight feathers of the chicken, goose, duck, white leghorn chicken, and emu; rhamphothecas of the chicken and emu; claws of the chicken, emu, and ostrich; and scales of the chicken and ostrich (detailed in *SI Appendix* and *SI Appendix*, Figs. S1–S4 and Table S1).

In this study, we demonstrate specific expressions of feather β-keratins and differentiate feather β-keratins from other β-keratins in numerous fossil taxa. These data shed light on the evolution of the proteinaceous components of feathers during the dinosaur–bird transition and provide a tool for assessing potential flight abilities in extinct feathered dinosaurs.

Results

Ultrastructural Nature of *Anchiornis* Feathers. Scanning electron microscopy (SEM) was used to compare the ultrastructure of pennaceous feathers attached to the forelimb of *Anchiornis* (Fig. 1 *A–D*) with flight feathers from the extant chicken, *Gallus gallus* (Fig. 1 *E* and *F*). SEM shows that feathers of *Anchiornis* are preserved as 3-dimensional filaments that are distinct from the sediment. In some regions of the feathers, microbodies that are morphologically similar to those previously identified as melanosomes (25) can be visualized within an amorphous matrix (Fig. 1*C*, yellow arrows). Chemical and molecular tests conducted here confirm this interpretation. Under higher magnification in SEM, the filamentous nature of these fossil feathers is more clearly visualized (Fig. 1*D*). At the same magnification, the surface of barbules of extant flight feather of the chicken shows fibrous bundles forming regularly arranged angles (Fig. 1*F*) that are not observed in fossil feathers (Fig. 1*D*). However, such differences could be explained by taphonomic effects (e.g., compression and degradation) or as a result of the differences in the keratin compositions, as shown in this work.

Transmission electron microscopy (TEM) observations of sectioned *Anchiornis* feathers (Fig. 2) complemented the results of SEM. TEM of extant feathers shows that electron-dense
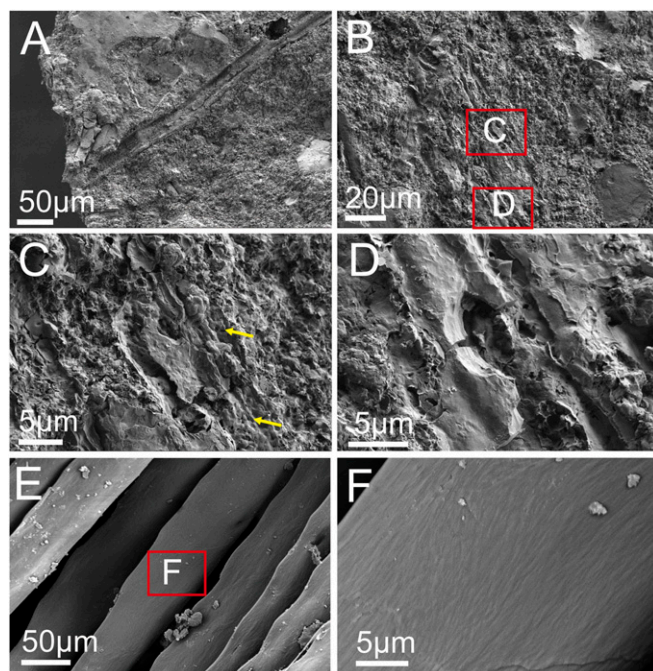

Fig. 1. SEM images of the sample from pennaceous feather attached to the right forelimb of *Anchiornis* compared with barbules of a black flight feather from the extant chicken *G. gallus*, showing that feathers of *Anchiornis* are preserved as 3D filaments. In some regions, melanosomes are embedded within the matrix as in extant feathers, but the microstructure of *Anchiornis* feathers differs from that of extant feathers, which could be caused by compression and degradation during the fossilization. (*A–D*) SEM images of a feather from *Anchiornis*; (*C* and *D*) High-magnification images of the boxed areas in *B*; melanosomes are indicated by yellow arrows. (*E* and *F*) SEM images of an extant feather from the chicken *G. gallus*; (*F*) High-magnification images of the boxed area in *E*.

melanosomes are embedded within a somewhat filamentous matrix that is less electron-dense (Fig. 2*A*). Similar electron-dense melanosomes were also visualized within a less electron-dense and filamentous matrix in *Anchiornis* feathers (Fig. 2*B*). The feathers from four additional, geologically younger specimens (Fig. 2 *C* and *G–I*) show the same ultrastructural pattern. However, at higher magnification, in addition to short and thin filaments ~3 nm in diameter (Fig. 2*E*, white arrow), the matrix of *Anchiornis* feathers is almost exclusively dominated by thick filaments ~8 nm in diameter (Fig. 2*E*, red arrow), which is not seen in flight feathers of extant birds, such as the chicken (Fig. 2*D*). In contrast, the matrix of the four younger fossil feathers is dominated by short and thin (~3–4 nm) filaments (Fig. 2 *F* and *J–L*), comparable to those observed in feathers of extant birds (Fig. 2*D*). Notably, we propose that the very dense arrangement of melanosomes in the fossil feathers (Fig. 2 *B*, *C*, and *G–I*, yellow arrows) does not reflect in-life distribution, but is, rather, a taphonomic response to postmortem or postburial compression (25).

Chemical Composition of *Anchiornis* Feather. We conducted ChemiSTEM analyses using an FEI Titan G2 series of Cs-corrected scanning/TEM (STEM) (26). We combined high-resolution elemental maps with detailed images of the ultrastructure of *Anchiornis* feathers and compared these with feathers from the four younger fossil specimens and a flight feather of *Gallus* (Fig. 3). The distributions of nitrogen, sulfur, copper, and calcium were mapped for each specimen. Differences in elemental composition can be used to differentiate ultrastructural components.

Sulfur and nitrogen are more prevalent in the keratin matrix of extant feathers than in the embedding LR White resin (Fig. 3 *B*
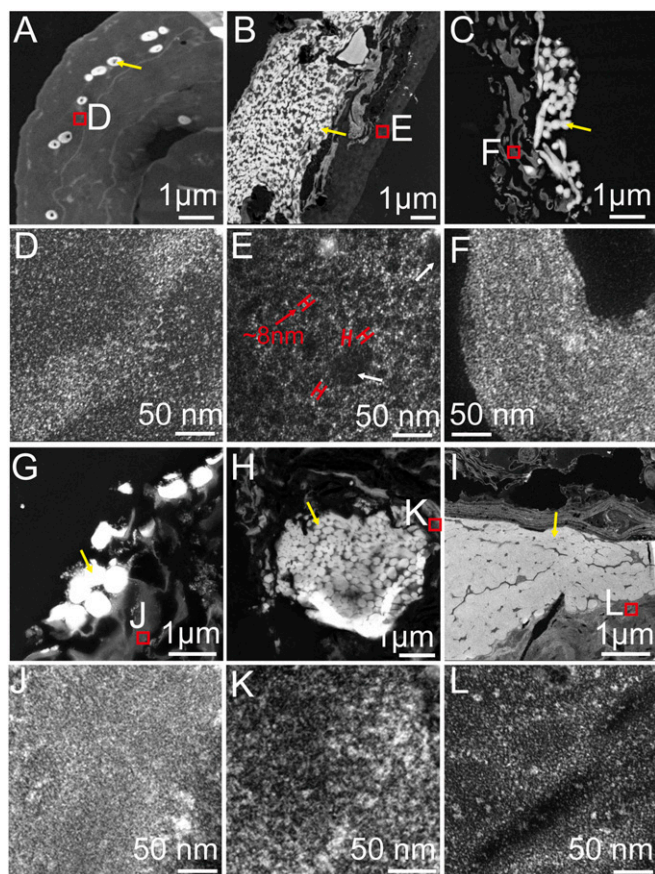
Fig. 2. TEM images showing that melanosomes are embedded within a matrix, but at a high resolution, the matrix is dominated by thick filaments in *Anchiornis* feathers unlike the other comparable fossil and extant feathers dominated by much thinner filaments. TEM images of a black flight feather from the extant chicken *G. gallus* (*A* and *D*) compared with the sample from a pennaceous feather attached to the right forelimb of *Anchiornis*, (*B* and *E*) the sample from a pennaceous feather possibly attached to the left forelimb of Dromaeosauridae indet., (*C* and *F*) The sample from a wing feather attached to the right forelimb of *Eoconfuciusornis*, (*G* and *J*) the sample from a tail feather near the distal end of the left pubis of *Yanornis*, (*H* and *K*) and the sample from the isolated Oligocene flight feathers (*I* and *L*). (Scale bars: *A–C*, *G*, and *I*, 1 μm; *D–F* and *J–L*, 50 nm.) Yellow arrows indicate melanosomes, white arrows indicate the short and thin filaments, red arrows indicate the thick filaments.

and *C*), and sulfur is more abundant in extant melanosomes than in either the keratin matrix or the embedding LR White resin (Fig. 3*C*). Copper and calcium are also detected in extant melanosomes, but are not seen in either the LR white resin or the keratin matrix surrounding these melanosomes (Fig. 3 *D* and *E*). In contrast, there is virtually no detectable difference in nitrogen concentration between the keratin matrix and the melanosomes (Fig. 3*B*).

Similarly, in all five fossil feathers, including those from *Anchiornis*, melanosomes exhibit higher concentrations of nitrogen, sulfur, copper, and calcium than either the surrounding matrix or the embedding LR White resin (Fig. 3 *G–J*, *L–O*, *Q–T*, *V–Y*, and *AA–AD*). The less electron-dense matrix shows nitrogen values that are slightly elevated relative to the embedding LR White resin, but significantly lower than those seen in melanosomes (Fig. 3 *G*, *L*, *Q*, *V*, and *AA*). The *Anchiornis* feather does not exhibit higher level of sulfur in the matrix compared with the LR White resin (Fig. 3*H*), in contrast to the feathers of the four younger fossils (Fig. 3 *M*, *R*, *W*, and *AB*). Combined with the ultrastructural observations obtained by SEM and TEM (Figs. 1 and

2), these data support the hypothesis that the matrix surrounding the melanosomes in *Anchiornis* feathers has preserved endogenous organic, nitrogen-containing materials (e.g., proteins). However, a reduced level of detectable sulfur in *Anchiornis* feathers indicates that the matrix dominated by thick filaments is different from that seen in younger fossils and extant feathers.

Molecular Compositions of *Anchiornis* Feathers. To characterize the molecular composition of feathers from all five fossil feathers, we capitalized on the demonstrated homology and variability of the β-keratin gene family, as well as on the specificity and sensitivity of the vertebrate immune system. The immunohistochemistry results were compared with the results from the same assays on the short, hollow fibers in *Shuvuuia*, the claw sheath from *Citipati*, and flight feathers and other cornified tissues from extant taxa, using the same parameters as employed with fossil materials, but tested in isolation to avoid cross contamination.

A polyclonal antiserum (universal anti-β-keratin antiserum) raised against extracts of mature white chicken feathers (27) was employed to detect β-keratin in situ in various fossil and extant tissues. This general antiserum reacts not only with feathers but also with other cornified tissues composed of sauropsid-specific β-keratin (27) (*SI Appendix*, Figs. S5 and S6 and Table S4). However, it differentiates β-keratin-containing tissues from those composed of α-keratins or other proteins (27, 28). Both immunofluorescence (IF) and immunogold (IG) labeling revealed the presence of specific epitopes consistent with β-keratins in *Anchiornis* feathers (Fig. 4 *G* and *K*), but with reduced avidity relative to that seen in extant feathers (Fig. 4*B*).

We then generated two synthetic peptides based on sequence data from extant feathers that correspond to unique regions of feather β-keratins (for antigen designs, see *SI Appendix*), and used these peptides to generate peptide-specific polyclonal antisera (*SI Appendix*, Table S2). We showed that these antisera specifically recognize feather β-keratins and, unlike the more general anti-β-keratin antiserum, do not cross-react with extant tissues expressing claw or scale β-keratins (*SI Appendix*, Figs. S5–S7 and Tables S3 and S4). These antipeptide antisera also reacted with *Anchiornis* feathers (Fig. 4 *H* and *I*) in a pattern similar to that seen in extant feathers (Fig. 4 *C* and *D*), which was confirmed using IG labeling (Fig. 4 *L* and *M*).

The two antipeptide antisera, together with the more general anti-β-keratin antiserum, were applied to the four younger fossil feathers, the short fibers from *Shuvuuia*, and the claw sheath from *Citipati*. As predicted, all younger fossil feathers reacted positively to all three antisera, but the short fibers from *Shuvuuia* and the claw tissue from *Citipati* reacted only to the more general anti-β-keratin antiserum and not to the two feather-specific antipeptide antisera (*SI Appendix*, Figs. S8 and S9). The results of IF and IG tests are consistent and provide support for the hypothesis that the epitopes specific to feather β-keratins are both expressed and preserved in the *Anchiornis* feathers (Fig. 4 *H*, *I*, *L*, and *M*). These data suggested that the *Anchiornis* feathers contain feather β-keratins, although the alternative interpretation that the *Anchiornis* feathers may contain a basal β-keratin that shares some of the epitopes of the two peptides specific to feather β-keratins (e.g., feather-like β-keratins) cannot be refuted.

Although showing positive immunoreactions to the general anti-β-keratin antiserum and the two feather-specific antipeptide antisera, at the ultrastructural level, *Anchiornis* feathers differ from feathers of extant birds by expressing not only the short and thin (3 nm) filaments consistent with β-keratin but also a greater number of thick filaments with a diameter about 8 nm, which are more consistent with basal α-keratins. This suggests that *Anchiornis* feathers expressed both α-keratins and feather β-keratins, a pattern seen in both embryonic and mature feathers of extant birds (17).
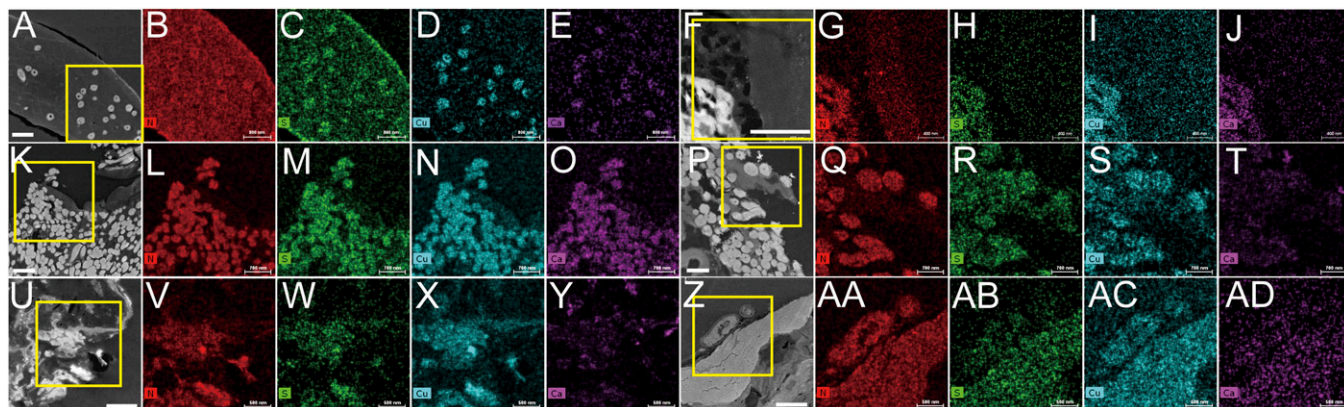
Fig. 3. Elemental maps of the ultrastructure of various fossil feathers compared with that of an extant feather of *G. gallus* in TEM images. Both extant and fossil feathers show similar elemental compositions of the melanosomes and surrounding matrix. With the exception of *Anchiornis*, the surrounding matrix does not show a high concentration of sulfur. TEM image and corresponding elemental maps of feather from the chicken *G. gallus* (*A–E*), *Anchiornis* (*F–J*), Dromaeosauridae indet. (*K–O*), *Eoconfuciusornis* (*P–T*), *Yanornis* (*U–Y*), and the isolated Oligocene feather (*Z–AD*). Boxes show areas selected for elemental mapping. Maps of nitrogen are red, maps of sulfur are green, maps of copper are blue, and maps of calcium are purple. (Scale bars: 1 μm.)

As discussed, ChemisTEM elemental maps showed that *Anchiornis* feathers had lower sulfur concentrations than the feathers of extant birds and the four younger fossils examined. Although various diagenetic influences on different fossil specimens cannot be ruled out, this low sulfur content is consistent with the hypothesis that the dominant structural protein in *Anchiornis* feathers is α-keratin, which contains fewer sulfur cross-links than feather β-keratin.

On the basis of these data, we hypothesize that if original α-keratins were preserved in the *Anchiornis* feathers, they would react with a general antiserum against α-keratins. Therefore, we obtained a mouse monoclonal antiserum to pan cytokeratin that exhibited broad α-keratin reactivity (AE1/AE3 +5D3; Abcam plc.; *SI Appendix*, Fig. S10). Both IF and IG labeling were consistent with the presence of the epitopes of α-keratin in the *Anchiornis* feathers (Fig. 4 *J* and *N*).

Although all three β-keratin antisera reacted with the *Anchiornis* feathers and the feathers of four younger fossils, only the feathers of *Anchiornis*, Dromaeosauridae indet., and the basal bird *Eoconfuciusornis*, as well as the claw sheath of *Citipati*, showed reactivity with the pan α-keratin antisera, in both IF and IG (*SI Appendix*, Figs. S8 and S11).

We employed a plethora of controls to validate these immunological results. For example, to test for spurious or nonspecific

binding of the secondary antibody, we eliminated incubation with the specific primary antibodies, but held all other steps identical (Fig. 4 *A*, *E*, and *F*). To test for nonspecific binding of the primary antibody, we saw no binding when feathers were exposed to a nonrelevant antibody (e.g., antipeptidoglycan monoclonal antiserum) used at the same concentration as the test serum (*SI Appendix*, Fig. S7). We also demonstrated that neither primary nor secondary antibodies bind to the sediment controls (*SI Appendix*, Fig. S12).

Discussion

Keratins have a higher preservation potential than most other proteins, largely because of their molecular structure (14, 29, 30). All keratins, but particularly β-keratins, incorporate many hydrophobic residues that exclude water and a high concentration of sulfur-bearing amino acids that facilitate intra- and intermolecular disulfide bond formation, which in turn confers and enhances stability (30). Hence, keratins resist degradation by most proteolytic enzymes (29) and are somewhat protected against hydrolysis, thereby enhancing their preservation potential over other nonbiomineralized tissues.

We have used multiple high-resolution analytical methods (SEM, TEM, ChemiSTEM), as well as IF and IG labeling, to

Fig. 4. In situ IF and IG using four antisera (against extracted feather proteins, Peptide 1, Peptide 2, and broad α-keratin, respectively) on the sample of the pennaceous feathers attached to the right forelimb of *Anchiornis* and the black flight feather from the chicken *G. gallus*. All three β-keratin antisera reacted positively with *Anchiornis* feathers, and in the same pattern as with the chicken feather, but the pan α-keratin antisera reacted only with *Anchiornis* feather. (*A* and *F*) Negative controls, where no primary antibody is applied but all other steps kept identical to test conditions (for additional controls see *SI Appendix*). (*B*, *G*, and *K*) Exposed to the more broadly cross-reactive antisera against extracted feather proteins. (*C*, *H*, and *L*) Incubated with antisera against feather-specific Peptide 1. (*D*, *I*, and *M*) Exposed to antisera against feather-specific Peptide 2. (*E*, *J*, and *N*) Tested against antisera to the broadly distributed α-keratin. (*B–E*) IF tests on *G. gallus* feathers. (*G–J*) IF tests on *Anchiornis* feathers. (*B–D* and *G–J*) Antibody–antigen (ab-ag) complexes localized to feather tissues from both *G. gallus* and *Anchiornis*. (*E*) Does not show binding to the antiserum against broad α-keratin. (*K–N*) IG tests on *Anchiornis* feathers show ab-ag localized to feather tissues. [Scale bars: (*A–J*), 20 μm; (*K–N*), 200 nm.]
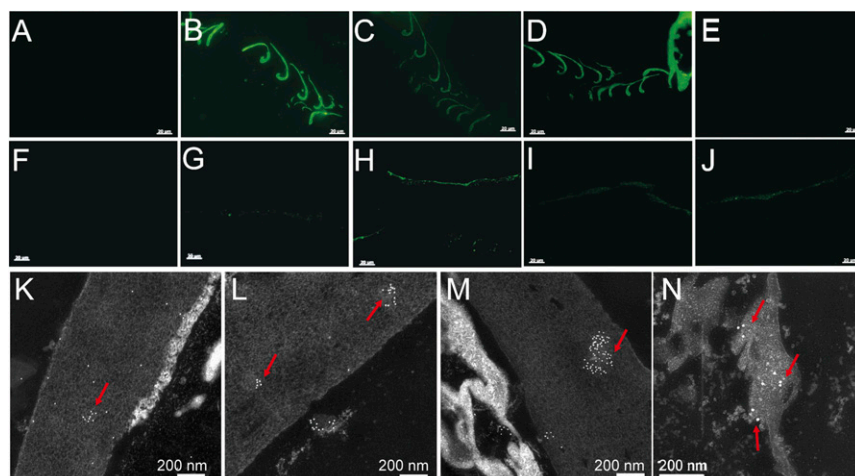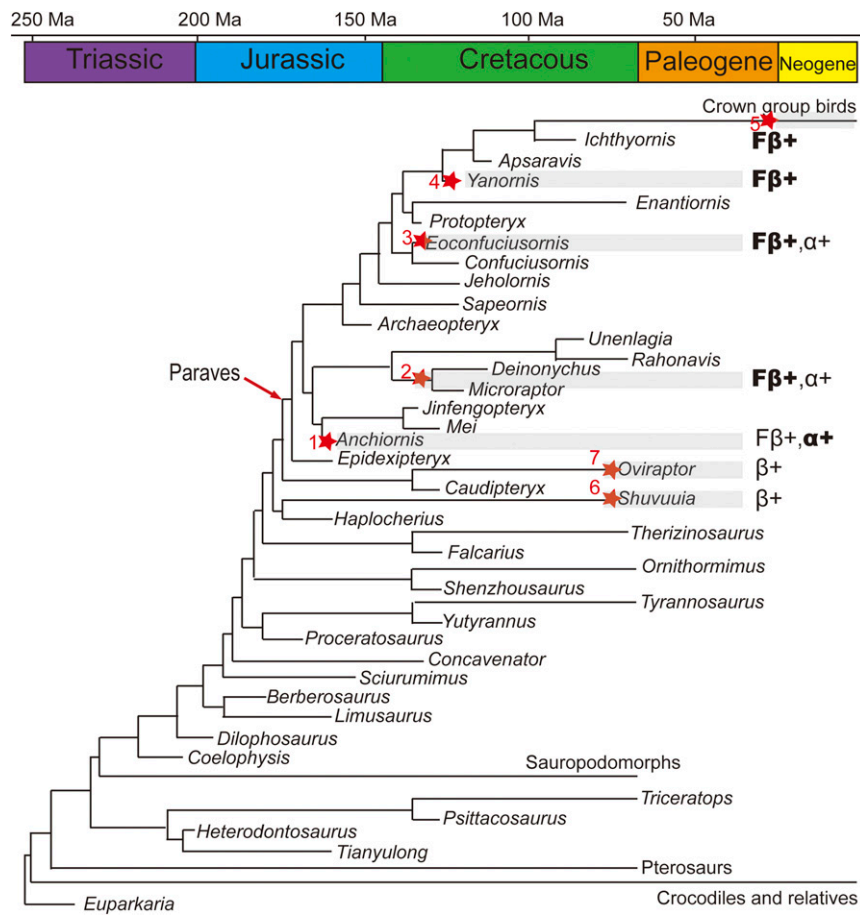
Fig. 5. Time-scaled evolution of molecular composition and ultrastructure of feathers within a simplified Mesozoic avian and nonavian phylogeny (38), suggesting that the *Anchiornis* feather were composed of both feather β-keratins and α-keratins, but dominated by α-keratins, unlike feathers from younger fossils and mature feathers of extant birds, which are dominated by β-keratins. Filled stars showing the distribution of tested fossil feathers and related integumentary tissues used in this study: (1) *Anchiornis* (STM 0–214), (2) Dromaeosauridae indet. (STM5-12), (3) *Eoconfuciusornis* (STM7-144), (4) *Yanornis* (STM9-5), (5) Isolated flight feather (DY 1502006), (6) *Shuvuuia deserti* (IGM 100/977), and (7) *Citipati* (MPC-D). β+, positive reaction to the general β-keratin antiserum; Fβ+, positive reaction to the antiserum specific feather β-keratins; α+, positive reaction to the anti-pan cytokeratin antiserum; "Fβ+" in bold, thin β-keratin filaments is dominant in ultrastructure; "α+" in bold, thick α-keratin filaments is dominant in ultrastructure.

investigate the protein composition of the feathers of *Anchiornis* by comparing them with materials from several related fossils and tissues from extant birds. Our study not only supports the presence of endogenous keratins in the fossil materials but also shows that specific antibodies, when combined with ultrastructural data, can be used to differentiate cornified tissues in feathers of extant and extinct birds and dinosaurs or other integumentary structures. We demonstrate that keratins within preserved integumentary structures can be identified in nonavian dinosaurs and birds, revealing potential biomechanical properties.

Our data support the hypothesis that feather β-keratins are coexpressed and preserved with more basal α-keratins in the *Anchiornis* fossil integumentary materials, but that α-keratins take the predominant position, which is clearly different from comparable flight feathers in extant birds. These molecular data are supported by ultrastructural data showing the presence of thick filaments resembling α-keratins in the *Anchiornis* feathers. Because mature feathers of extant birds are dominated by feather β-keratins, the coexpression of α-keratins and feather β-keratins, in combination with the ultrastructural patterns shown here, suggests that feathers of *Anchiornis* may represent an evolutionary transition between more ancestral integumentary appendages and extant bird feathers. Subsequent predominance of feather β-keratins in mature feathers of extant birds have been shown to greatly affect the mechanical properties, increasing resilience and

plasticity (13, 14). Thus, these modifications may have evolved in tandem with the evolution of powered flight.

Several genomic studies indicate that feather β-keratin genes were probably present in the genome and expressed in the epidermis of scaled archosaurians and lepidosaurs before the emergence of feathers (31–34). However, the formation of feather placodes and the origin of the axial rachis and hierarchical branching of barbs and barbules, as well as different feather types with different functions, required increasing specialization of the feather β-keratin genes (15). This is reflected by both a reduction in the number of α-keratin genes and a significant expansion of β-keratin genes in the bird genomes relative to those in mammals and reptiles (19, 35), thus indicating that β-keratin gene duplications and mutations may be linked to feather evolution and adaptations of birds to different ecological niches (19, 20, 36, 37).

Thus, at the molecular and ultrastructural levels, the pennaceous feathers of *Anchiornis* may represent an intermediate stage in feather evolution. In *Anchiornis*, thin filaments of feather β-keratins are not yet widely distributed, nor have the thick filaments of α-keratin been superseded by successive β-keratin expression in this ancient paravian. The molecular composition and ultrastructure of *Anchiornis* feathers suggest that their pennaceous feathers may have lacked the biomechanical properties suitable for flight, unlike mature feathers of extant birds.

When these data are considered within the well-established phylogenetic framework of Aves and their closest relatives (38) (Fig. 5), we conclude that specific feather β-keratins most likely evolved outside the clade Aves, being expressed in the feathers of paravians (e.g., *Anchiornis*); basal α-keratin coexpression is retained in at least some paravian feathers; and although the feathers of the Early Cretaceous nonavian dinosaurs (e.g., Dromaeosauridae indet.) and basal birds (e.g., *Eoconfuciuornis*) also coexpressed feather β-keratins and α-keratins, they were more similar at the ultrastructural levels to the feathers of more derived birds (e.g., *Yanornis*), including neornithines, which demonstrate an absence of observable thick filaments composed of α-keratins. Therefore, we hypothesize that feathers continued to evolve throughout the Cretaceous until they reached the condition in Neornithes in which feather β-keratins predominated, thereby producing flexible and resilient feathers suitable for powered flight. Our data also suggest a mosaic pattern in the evolution of protein expression in dinosaurs that are closely related to birds. For example, *Shuvuuia* fibers show reactivity to the general β-keratin antiserum, but do not show evidence of the deletion event specific to feathers. However, the *Shuvuuia* fibers lost the coexpression of α-keratin, whereas *Anchiornis* feathers expressed the feather β-keratins together with α-keratins, as is observed in other cornified sauropsid tissues.

This study not only confirms the preservation of endogenous keratins in various Mesozoic and Cenozoic fossil materials but also demonstrates the possibility of conducting rigorous molecular studies to address the relative timing of molecular events in cornified tissues. It also highlights the importance of integrating morphological, developmental, and molecular data (including those directly from fossils) in proposing and testing evolutionary hypotheses. However, to achieve a statistical significance of such studies, greater access to fossil materials and, particularly, to those with better preservation is needed.

Materials and Methods

Experimental procedures for sampling, electron microscope observation, ChemiSTEM elemental mapping, in situ immunohistochemistry, and strict controls are described in SI Appendix, Materials and Methods.

1. Chen P-J, Dong Z-M, Zhen S-N (1998) An exceptionally well-preserved theropod dinosaur from the Yixian formation of China. *Nature* 391:147–152.
2. Qiang J, et al. (1998) Two feathered dinosaurs from northeastern China. *Nature* 393:753–761.
3. Hu D, Hou L, Zhang L, Xu X (2009) A pre-*Archaeopteryx* troodontid theropod from China with long feathers on the metatarsus. *Nature* 461:640–643.
4. Zheng X-T, You HL, Xu X, Dong ZM (2009) An early Cretaceous heterodontosaurid dinosaur with filamentous integumentary structures. *Nature* 458:333–336.
5. Godefroit P, et al. (2014) Dinosaur evolution. A Jurassic ornithischian dinosaur from Siberia with both feathers and scales. *Science* 345:451–455.
6. Mayr G, Peters DS, Plodowski G, Vogel O (2002) Bristle-like integumentary structures at the tail of the horned dinosaur Psittacosaurus. *Naturwissenschaften* 89:361–365.
7. WANG LL, et al. (2013) SIMS U-Pb zircon age of Jurassic sediments in Linglongta, Jianchang, western Liaoning: Constraint on the age of oldest feathered dinosaurs. *Chin Sci Bull* 58:1346.
8. Mayr G, Pohl B, Peters DS (2005) A well-preserved *Archaeopteryx* specimen with theropod features. *Science* 310:1483–1486.
9. Xu X, You H, Du K, Han F (2011) An *Archaeopteryx*-like theropod from China and the origin of Avialae. *Nature* 475:465–470.
10. Wang X, et al. (2017) Basal paravian functional anatomy illuminated by high-detail body outline. *Nat Commun* 8:14576.
11. Evangelista D, et al. (2014) Aerodynamic characteristics of a feathered dinosaur measured using physical models. Effects of form on static stability and control effectiveness. *PLoS One* 9:e85203.
12. Zhang F-C, Zhou Z-H, Gareth D (2006) Feathers and 'feather-like' integumentary structures in Liaoning birds and dinosaurs. *Geol J* 41:395–404.
13. Fraser RDB, Parry DAD (2011) The structural basis of the filament-matrix texture in the avian/reptilian group of hard β-keratins. *J Struct Biol* 173:391–405.
14. Fraser RDB, Parry DAD (2014) Amino acid sequence homologies in the hard keratins of birds and reptiles, and their implications for molecular structure and physical properties. *J Struct Biol* 188:213–224.
15. Alibardi L (2017) Review: Cornification, morphogenesis and evolution of feathers. *Protoplasma* 254:1259–1281.
16. Alibardi L, Toni M (2008) Cytochemical and molecular characteristics of the process of cornification during feather morphogenesis. *Prog Histochem Cytochem* 43:1–69.
17. Wu P, et al. (2015) Topographical mapping of α- and β-keratins on developing chicken skin integuments: Functional interaction and evolutionary perspectives. *Proc Natl Acad Sci USA* 112:E6770–E6779.
18. Gregg K, Rogers GE (1986) Feather keratin: Composition, structure and biogenesis. *Biology of the Integument: 2 Vertebrates*, eds Bereiter-Hahn J, Matoltsy AG, Richards KS (Springer, Berlin), pp 666–694.
19. Greenwold MJ, et al. (2014) Dynamic evolution of the alpha (α) and beta (β) keratins has accompanied integument diversification and the adaptation of birds into novel lifestyles. *BMC Evol Biol* 14:249.
20. Greenwold MJ, Sawyer RH (2010) Genomic organization and molecular phylogenies of the beta (beta) keratin multigene family in the chicken (Gallus gallus) and zebra finch (Taeniopygia guttata): Implications for feather evolution. *BMC Evol Biol* 10:148.
21. Glenn TC, French JO, Heincelman TJ, Jones KL, Sawyer RH (2008) Evolutionary relationships among copies of feather beta (beta) keratin genes from several avian orders. *Integr Comp Biol* 48:463–475.
22. Greenwold MJ, Sawyer RH (2011) Linking the molecular evolution of avian beta (β) keratins to the evolution of feathers. *J Exp Zoolog B Mol Dev Evol* 316:609–616.
23. Greenwold MJ, Sawyer RH (2013) Molecular evolution and expression of archosaurian β-keratins: Diversification and expansion of archosaurian β-keratins and the origin of feather β-keratins. *J Exp Zoolog B Mol Dev Evol* 320:393–405.
24. Hu D, et al. (2018) A bony-crested Jurassic dinosaur with evidence of iridescent plumage highlights complexity in early paravian evolution. *Nat Commun* 9:217.
25. Pan Y, et al. (2016) Molecular evidence of keratin and melanosomes in feathers of the early Cretaceous bird *Eoconfuciusornis*. *Proc Natl Acad Sci USA* 113:E7900–E7907.
26. Pan Y-H, Hu L, Zhao T (2018) Applications of chemical imaging techniques in paleontology. *Natl Sci Rev*, 10.1093/nsr/nwy107.
27. Moyer AE, Zheng W-X, Schweitzer MH (2016) Microscopic and immunohistochemical analyses of the claw of the nesting dinosaur, Citipati osmolskae. *Proc R Soc B Biol Sci* 283:20161997.
28. Lindgren J, et al. (2017) Biochemistry and adaptive colouration of an exceptionally preserved juvenile fossil sea turtle. *Sci Rep* 7:13324.
29. Sharma S, Gupta A (2016) Sustainable management of keratin waste biomass: Applications and future perspectives. *Braz Arch Biol Technol* 59:e16150684.
30. Yin X-C, et al. (2013) Study on effective extraction of chicken feather keratins and their films for controlling drug release. *Biomater Sci* 1:528.
31. Sawyer RH, Knapp LW (2003) Avian skin development and the evolutionary origin of feathers. *J Exp Zoolog B Mol Dev Evol* 298:57–72.
32. Sawyer RH, Rogers L, Washington L, Glenn TC, Knapp LW (2005) Evolutionary origin of the feather epidermis. *Dev Dyn* 232:256–267.
33. Sawyer RH, Washington LD, Salvatore BA, Glenn TC, Knapp LW (2003) Origin of archosaurian integumentary appendages: The bristles of the wild Turkey beard express feather-type β keratins. *J Exp Zoolog B Mol Dev Evol* 297:27–34.
34. Alibardi L, Dalla Valle L, Toffolo V, Toni M (2006) Scale keratin in lizard epidermis reveals amino acid regions homologous with avian and mammalian epidermal proteins. *Anat Rec A Discov Mol Cell Evol Biol* 288:734–752.
35. Vandebergh W, Bossuyt F (2012) Radiation and functional diversification of alpha keratins during early vertebrate evolution. *Mol Biol Evol* 29:995–1004.
36. Zhang G, et al.; Avian Genome Consortium (2014) Comparative genomics reveals insights into avian genome evolution and adaptation. *Science* 346:1311–1320.
37. Ng CS, et al. (2014) Genomic organization, transcriptomic analysis, and functional characterization of avian α- and β-keratins in diverse feather forms. *Genome Biol Evol* 6:2258–2273.
38. Xu X, et al. (2014) An integrative approach to understanding bird origins. *Science* 346:1253293.